

Science White Paper for LSST Deep-Drilling Field Observations Opportunities for Solar System Science

Authors: A.C. Becker (U. Washington), C.A. Trujillo (Gemini Observatory), R.L. Jones (U. Washington), N.A. Kaib (CITA), D. Ragozzine (SAO), S.T. Ridgway (NOAO), *and* the LSST Solar System Science Working Group

Contact Information for Lead Author/Authors: Andrew Becker, Astronomy Dept., University of Washington, Box 351580, Seattle WA 98195-1580; becker@astro.washington.edu; 206 685 0542

1 Science Goals

1.1 Concise List of Main Science Goals

Deep drilling sequences optimized for detecting small moving objects in our Solar System will increase our limiting magnitude from $r = 24.5$ in a single visit to $r = 27.0$. The “shift-and-stack” (SAS) method will be used to recover moving objects below the detection limit in single images. This increase in sensitivity will enable the following science, novel to LSST given the breadth and depth of the proposed observing sequence:

1. Extend the measurement of the size distribution of Solar System bodies a factor of 3 times smaller than in the Universal Cadence (UC). This will permit measurement of any roll-over in the size distributions of Trans-Neptunian Objects (TNOs), Neptune Trojans, Main belt asteroids (MBAs) and Jupiter Trojans, which would be indicative of collisional (versus accretional) growth. This will also allow us to directly study MBA precursors of Near Earth Asteroids (NEAs).
2. Measure the orbital distribution of TNOs and Neptune Trojans at the faint end of this size regime to search for changes as a function of size, constraining models of Solar System formation and evolution such as the Nice model (Tsiganis et al., 2005).
3. Identification of unique and unusual objects, such as Sedna population members, precursors to long period comets, very distant large objects, and main belt comets at fainter magnitude limits than in the main survey. Deep drilling allows us to identify these objects up to 2 times further away compared to the UC, or to identify surface emission or other extended features at a much higher signal-to-noise.

This science will be realized through a specialized deep drilling sequence optimized for Solar System objects. We propose imaging a set of 3×3 LSST fields centered along the ecliptic in latitude, and centered in longitude on a conjunction of the Jupiter and Neptune Trojan clouds (so as to achieve maximum depth on both of these populations with one set of DD fields). The first observation of these fields will occur at a time when the main belt asteroids in those fields are near their leading stationary points, approximately 1.5 months before opposition. A re-visit will happen within 2–3 days of the first observation of each field to provide acceleration vectors. This combination of observations defines a re-visit sequence. A second re-visit sequence will be acquired near opposition, and a third near the trailing stationary point in the main belt orbits, 1.5 months after opposition. A fourth re-visit sequence will occur near opposition in the subsequent year, yielding a total of 8 partial nights spent imaging each field.

In this series of observations, we will acquire 4 different snapshots of the main belt population, as most bodies will have moved out of the 3×3 area between each re-visit sequence. Accordingly these

objects will *not* have well-determined orbital parameters. However, we will have well-established brightness distributions, with sufficient amounts of data to translate this into a size distribution. Most TNOs will not have moved out of the imaging area, meaning we will be able to establish orbital parameters for these objects with the overall sequence of 8 per-field visits, each to $r = 27.0$, over 86 square degrees.

1.2 Details of Main Science Goals

1.2.1 Size Distribution of Main Belt Asteroids

The size distribution of asteroids is one of most significant observational constraints on their history and is considered to be the “planetary holy grail” (Jedicke & Metcalfe, 1998, and references therein). It is also one of the hardest quantities to determine observationally because of strong selection effects in the extant catalogs. Current Solar System catalogs (e.g. ASTORB) are complete only to limiting magnitude $r = 19.5$ (Parker et al., 2008). LSST will produce a moving object catalog complete to a limit 5 magnitudes fainter through its Universal Cadence (UC) alone.

Deep drilling (DD) cadences plus SAS will extend this detection limit to objects with diameters a factor of 3 times smaller than the single (Universal Cadence) exposure depth, enabling science in a different size regime than available through UC data. For example, the size distribution of MBAs is known to have significant structure that records the intrinsic strength of asteroids (e.g., O’Brien & Greenberg, 2005), and probing to this size regime will allow studies of the global internal properties of asteroids.

Additionally, small MBAs are the direct predecessors of NEAs, migrating from the Main Belt into Near Earth orbits. A study of the MBA-NEA connection is only possible with both an NEA survey *and* a very deep MBA survey. Current dynamical models and orbit integrations (Bottke et al., 2002) suggest that NEAs are delivered primarily from specific regions within the Main Belt that are particularly affected by certain secular and mean-motion resonances. A key to understanding the transfer of MBAs into near-Earth orbital space is to determine the population of both classes, especially in the same size range as some processes (such as the Yarkovsky effect) influence small objects differently than larger objects. Presently, we only know the size frequency distribution (SFD) of MBAs down to a size of several km diameter. Unfortunately, only the largest hundred or so NEAs are that large, so there is very little overlap of our measured SFD of NEAs with that of MBAs.

By the time LSST begins operations, nearly all of the NEAs with diameters greater than 1 km will have been cataloged by surveys such as Pan-STARRS. At smaller sizes, LSST will inventory 90% of all NEAs down to 150m in diameter in the main UC survey, and detect 90% of all MBAs larger than 400m. Extending the detection of MBAs to ~ 150 m will require deep observing sequences, but will dramatically improve our understanding of the direct precursors of those NEAs.

1.2.2 Orbital Distribution of TNOs

In recent years, the Nice model (Tsiganis et al., 2005) has proposed that all giant planets formed at less than 14 AU from the Sun and the solar nebula was truncated near 30 AU. The giant planets and small bodies in the Solar System subsequently evolved to their current state through planetary migration due to angular momentum exchange with planetesimals. The Nice model presents an intriguing theory which could account for many previously unexplained problems in various small body populations. However, the Nice model has problems reproducing the orbital distribution (particularly the eccentricities and inclinations) of the classical Kuiper Belt. Competing models of Solar System evolution (such as rogue planetary embryos sculpting the primordial Kuiper belt (Gladman & Chan, 2006), smooth migration of Neptune (Hahn & Malhotra, 2005), or a stellar flyby

(Kenyon & Bromley, 2004)) each have their own problems reproducing the observed distribution of TNOs. Better measurements of both the size and orbital distributions of TNOs, particularly at the very small size regime where it appears that these distributions are different than at ~ 400 km sizes, will provide much stronger tests of these models.

In particular, current observations show that the inclination distribution and size distribution of the cold Classical belt is different than the dynamically excited “hot” components of the Kuiper Belt (e.g. Bernstein et al., 2004; Gulbis et al., 2010; Fraser et al., 2010). The cold Classical belt is typically composed of smaller, redder, and less dynamically excited (and thus lower inclination) objects. Other work by Noll et al. (2008) has found a different binary fraction for cold Classical belt objects than for higher inclination, “hot” TNOs; Parker & Kavelaars (2010) suggests this may be a result of the high-inclination population scattering off Neptune during the giant planet’s migration. In the Nice model, both of the cold Classical belt and the more dynamically excited “hot” populations of objects would be implanted into the Trans-Neptunian region by the migration of Neptune; these observations seem to be indicating that the cold belt formed in situ instead.

Current surveys have been limited to either pencil beam surveys over extremely small areas with deep limiting magnitudes (less than a square degree to $R = 26$) and no followup observations to measure orbits, or wide field surveys over a few hundred square degrees to $R = 23$ with some surveys obtaining orbital measurements and others not expending the followup time. Extrapolating Bernstein et al. (2004) (the faintest survey for TNOs to date, covering 0.12 square degrees to $R = 28.7$) suggests that a single LSST field on the ecliptic would discover around 450 TNOs down to a limiting magnitude of $r = 27$. As LSST can cover many square degrees with each DD field, we can also follow almost *all* of these discovered objects over 2 years to determine their orbital parameters. With deep drilling fields plus the UC, LSST will dramatically improve the sample size of both large and small TNOs while also measuring their orbital distributions.

1.2.3 Understanding Trojan Populations

Studying the Trojan populations of Jupiter and Neptune also provides useful constraints on the environment of the early Solar System and its evolution over time. Currently there are no known Saturn or Uranus Trojans, despite some searches (e.g. Barbieri et al., 2005), though these are potentially stable for the age of the Solar System (e.g. Dvorak et al., 2010), thus we have not included these in considering DD field placement.

The origin of Jupiter’s large population of Trojans is not well understood. One hypothesis for the origin of the Trojans is that they were formed simultaneously with Jupiter and then captured and stabilized near the growing Jupiter’s L4 and L5 Lagrange points (Peale, 1993). An alternative hypothesis suggests they were captured over a much longer period after forming elsewhere in the Solar System (Jewitt, 1996). The colors of many known Trojans are similar to scattered disk objects from the outer Solar System and others appear similar to the colors of outer MBAs, lending support to the second hypothesis, with implications for the importance of gas drag in the early Solar System. The Nice model suggests a more complex picture, where the present permanent Trojan population is built up by planetesimals trapped after the 1:2 mean-motion resonance crossing of Saturn and Jupiter (Morbidelli et al., 2005). Jupiter Trojans are likely to move out of our DD fields before the proposed 1.5 month re-visit sequence (although they will be detectable in both nights within each re-visit), thus although we cannot measure their orbital distribution in the DD fields, we can measure their size distribution at sub-kilometer diameters to high precision. This will provide new constraints for these models, indicating whether the capture mechanism must depend on size.

The Neptune Trojans remain a particularly enigmatic population. The basic estimate of their numbers comes from the work of Sheppard & Trujillo (2006), who detected 6 Neptune Trojans in a survey of 49 square degrees to limiting magnitude 25.7. The size distribution of the Neptune Trojans is of fundamental interest, and suggests a roll-over to a flatter slope for the faintest bodies

in a manner similar to the TNOs (Sheppard & Trujillo, 2010) and MBAs, suggesting a similar planetesimal formation mechanism. These objects, being as distant as the inner Kuiper belt objects, will remain in our DD fields throughout the entire re-visit sequence, thus we can measure their orbital distribution in addition to their size distribution. Their orbital distribution is particularly interesting as a constraint on Neptune’s migration over the age of the Solar System (Lykawka et al., 2009).

In Table 1 we use the faint KBO size distribution to estimate the total population of likely Neptune Trojans. The Neptune Trojans can only be observed near Neptune’s L4 or L5 Lagrangian points, which lead/trail Neptune by 60 degrees on the sky. The Jupiter Trojans are similar, but have a wider distribution in ecliptic longitude. None of the other populations (MBAs or TNOs) have such significant longitudinal constraints.

1.2.4 Characterizing the Oort Cloud: Unusual and unique objects

Because the Oort Cloud is so remote, it is largely sculpted by perturbations outside the Solar System. Consequently, characterizing this reservoir provides clues about the Solar System’s environmental history. For instance, the size and orbital structure of the Sedna population as well as the rest of the Oort Cloud are intimately linked to the Sun’s birth environment (Brasser et al., 2006). In addition, these populations are also sensitive to the Sun’s dynamical history within the Milky Way after it left its birth cluster (Kaib et al., submitted). Lastly, there are two different models to explain the Oort Cloud’s formation. One predicts it is comprised of captured extrasolar bodies (Levison et al., 2010), while the other predicts that Oort Cloud bodies are native planetesimals that were scattered outward during and after giant planet formation (Oort, 1950). Better constraints on the Oort Cloud could discriminate between these two models.

The most recognizable known Inner Oort Cloud object is Sedna, which has the largest perihelion of any known body in the Solar System (76 AU; Brown et al., 2004). There are a few bodies with smaller perihelia that may be Inner Oort Cloud objects, but for the purposes of this document, we base our population estimates on Sedna itself. Sedna was found in the Caltech wide area survey (Trujillo & Brown, 2003), which has covered the available sky from Palomar (30,000 square degrees) to magnitude 20.7 and a more recent survey of 12,000 square degrees to 21.3 (Schwamb et al., 2010). With this one body, very limited information is available. However, Sedna’s extreme orbit out to 1000 AU places it out of the detection limit of either survey mentioned above for 99% of its orbit, suggesting that the total population of Inner Oort Cloud bodies could rival that of the Kuiper Belt itself. This population is of extreme importance because it represents one of our only links between currently observable bodies and the Oort cloud, a reservoir that is unlikely to be observable in our lifetimes and that may contain substantial mass that was ejected during the planet forming era of our Solar System.

While Sedna’s orbit is fossilized and unevolving, more distant Oort Cloud orbits are dynamic, and new bodies are continuously injected into planet-crossing orbits under the action of passing stars and the Galactic tide. This process produces the long-period comets (LPCs) observed near Earth, and they comprise a second observational constraint on the Oort Cloud. Although LPCs in the inner Solar System are relatively rare, their numbers should increase greatly beyond the orbits of Jupiter and Saturn (Kaib & Quinn, 2009). These objects are thought to sample a different source region of the Oort Cloud than nearby LPCs, thus providing new constraints on the distribution of objects in the Oort Cloud. The DD fields of LSST have the potential to detect and characterize this largely unknown population by detecting objects to distances about a factor of 2 greater than the UC fields.

1.3 Supplementary Science

1.3.1 Low Surface-Brightness Profiles of Comets

Traditionally, comets were thought to “turn off” beyond 3 AU, but in recent years that paradigm has started to change as we observe low but definitely non-zero mass loss from comets all the way to aphelion in the case of JFCs (e.g., Snodgrass et al., 2008; Mazzotta Epifani et al., 2008), and out beyond 25 AU in the case of Hale-Bopp (Szabó et al., 2008). LSST’s 10-year lifespan and deep magnitude limit will allow us to monitor many comets for outgassing activity over a significant interval of time (and for JFCs, over all or nearly all their orbits). The excellent spatial resolution will let us monitor even low levels of activity using point spread function comparisons, where the comet shows some coma that extends just slightly beyond the seeing disk. LSST will also be able to address how long comets stay active after perihelion and for what fraction of comets is crystallization of water ice and/or supervolatile sublimation a source of energy at high heliocentric distances. Deep drilling will significantly increase our ability to recover the surface brightness of comet comae.

It will also help in the identification of objects on MBA orbits exhibiting cometary activity. Such main belt comets (MBCs; e.g. Hsieh, 2007) are a recently discovered unusual population within the Main Belt Asteroids (MBAs). These bodies exhibit temporary coma on the order of weeks to months and are otherwise indistinguishable from other MBAs. The MBC population is of extreme interest since this could represent a significant source of water close to the Earth, possibly the source of the Earth’s own water. Since deep depths are required to detect outgassing, the LSST should greatly increase the total sample size of the known MBCs (currently only several are known). In addition, important characteristics such as the duration of the outgassing can be estimated, as well as explorations of orbital characteristics, such as whether the outgassing preferentially occurs near perihelion. The MBCs present a difficult logistical complexity because of their fast motion. Both of these tasks become easier if MBAs are searched for near their stationary points. We will use the need to recover these rapidly moving objects at faint magnitudes to motivate observations when they are at stationary points in their orbits. This will ensure that they remain in the field during the 2–3 day revisit timescale, as well as minimize the number of trajectories that need to be examined through SAS.

1.3.2 Time Variability

For objects which are visible in each individual frame (and thus would also be detectable in the main UC survey), we can use the dense time coverage of the DD observations to provide strong constraints on their time variability. This time variability can arise due to shape elongation or variations in surface composition, thus can provide valuable information about the physical properties of individual objects, from MBAs to TNOs.

Objects as distant as the Kuiper belt go through only a very small change in phase angle throughout the time they are visible, thus from observing TNOs in the DD and UC fields we may only derive rotational periods. From rotational periods only, a 2-dimensional estimate of the elongation of the object is possible, providing some constraints on the material strength of the TNO. By measuring the distribution of rotational periods, we can place constraints on the collisional history of the Kuiper belt. Much of this science can be obtained from the UC data alone, however the better time resolution of the DD fields will improve the rotation period estimates dramatically for the objects within these pointings.

Objects closer to Earth, such as the MBAs, NEAs and Jupiter Trojans, present a wider variety of phase angles and thus a combination of sparse observations from the UC survey plus the very dense time coverage of the DD fields can provide much more information on the full 3-dimensional shape of these objects. We will be able to determine not just their rotation period, but also the

rotation axis orientation (spin axis) and perhaps a full 3-D shape model through sparse lightcurve inversion for tens of thousands of MBAs, NEAs and Jupiter Trojans.

Asteroidal rotation and the direction of its spin axis are an obvious consequence of the accretion and collision process. On the order of a few thousand asteroids have reliably measured rotation rates – Harris & Pravec (2006) provide a brief overview on asteroid rotational periods, which range from 2 hours up to about a day, with brightness variations ranging from less than 0.2 magnitudes to over a magnitude, reflecting tensile strengths and rubble pile or monolithic structures. Kryszczyńska et al. (2007) point to an online catalog of asteroid spin states and pole positions, illustrating a non-random distribution of pole axis positions likely due to radiation pressure torques. Kaasalainen & Torppa (2001) and Kaasalainen et al. (2001) have shown that several hundred accurate phase data are sufficient to support optimal inversion of lightcurves to determine shape distributions. With the LSST DD fields, we will be able to dramatically increase the sample size of asteroids with known spin states and pole positions (and even full 3-D shape models).

2 Description of Proposed LSST Observations

We propose a contiguous area of 9 LSST fields for our deep drilling sequence, arranged in a 3×3 grid. The central field will be chosen at ecliptic latitude of zero, and an ecliptic longitude that contains a conjunction of the Trojan clouds of Jupiter and Neptune (of which several occur during the planned course of LSST). Each field will be imaged with 4 re-visit sequences, defined as two field visits separated by 2–3 nights. Each visit is assumed to be a continuous sequence of 15s exposures, each separated by 2s of shutter and readout. Optimally all data will be taken in the r -band filter; however, observations in g -band would also be acceptable if this would enable additional non-Solar System science. To achieve a limiting magnitude of $r = 27.0$ at 7σ requires 336 images be taken per night. The total time requested for 8 total visits to our 9 Solar System DD fields is 24,192 observations, or 114 hours of observations.

Revisit sequences will be arranged as follows:

- Revisit 1: To coincide with the stationary points in the orbits of main belt asteroids (and MBCs). Figure 1 shows the apparent sky motions for objects as a function of distance from opposition. For main belt objects (~ 2 AU) this occurs around 45 deg, or 1.5 months, from opposition. The Jupiter Trojan objects at 5 AU will have significant motion over the sequence, while the Neptune Trojan objects and TNOs will have slight motion. Observing at this point will provide for significant depth of detection for MBCs. A repeat set of observations 2–3 nights subsequent, completing the first revisit sequence, will provide for acceleration vectors, and thus distance estimates.
- Revisit 2: To coincide with opposition for these fields. As Figure 1 shows, observations at opposition provide very strong distance estimates from apparent motion alone.
- Revisit 3: To coincide with the second stationary points in the orbits of main belt asteroids, 1.5 months after opposition.
- Revisit 4: To coincide with opposition for these field centers, but taken a year after field Revisit 2. This will nail down the orbits of TNOs in the field. Both field revisits 2 and 4 will be very useful for determining the stellar background in these fields down to $r = 27.0$ (since the numerous main belt objects will be nearly stationary in revisits 1 and 3).

Because the objects we wish to observe are constantly in motion, we must choose between competing conditions. On one hand, objects at stationary points in their orbits are easier to recover

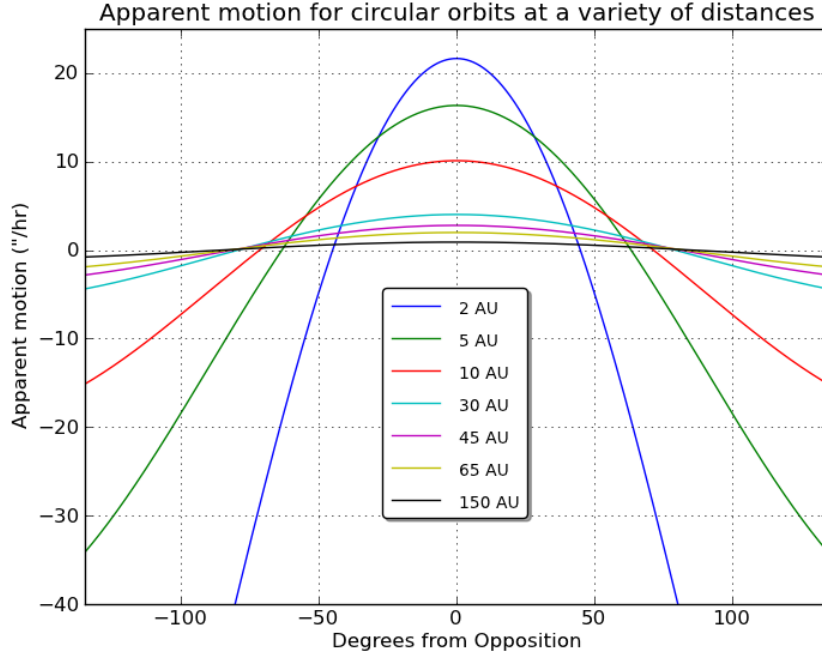


Figure 1: Illustration showing the apparent sky motion of bodies on circular orbits as a function of angle from opposition (defined as when the Sun and reference point are separated by 180 degrees on the sky), for objects at a variety of different semi-major axes. Stationary points are when curves cross apparent motion of zero.

using SAS; however they are only partially illuminated, and thus will appear fainter than at opposition. In these cases, distances are best estimated using velocity and acceleration. On the other, objects at opposition are at their brightest (being fully illuminated) and their distances may be inferred directly from their velocities. Bracketing these conditions is the need to obtain observations of TNOs over several months to constrain their orbits. We feel that this proposal to include both stationary point observations and opposition observations enables the bulk of the science above, for both the rapidly moving MBCs and slowly moving TNOs.

For pure number statistics, field locations on or near the ecliptic are preferred since that is where the bulk of the objects reside. However, fields far off the ecliptic are also useful for finding highly inclined objects like the Inner Oort Cloud objects, a consideration for selection of DD field centers that do not move (e.g. for supernova science). In general, fields should be away from the Galactic plane to reduce confusion and background noise. Finally we request contiguous fields parallel to the ecliptic to track any distant objects moving field-to-field.

2.1 List of Proposed Fields

We propose a Solar System-optimized deep drilling region, composed of 3×3 contiguous fields centered on the ecliptic and spanning a small range of ecliptic latitudes. We will choose the starting ecliptic longitude β_0 to coincide with the conjunction of Trojan populations of the giant planets (these clouds are likely to be quite extended, > 10 deg, so even a "near-conjunction" is still valuable). These include:

- $\beta_0 = 283$ deg on 2018-04 (Jupiter L4 and Neptune L5)
- $\beta_0 = 54$ deg on 2022-04 (Jupiter L4 and Neptune L4)

- $\beta_0 = 292$ deg on 2022-07 (Jupiter L5 and Neptune L5)
- $\beta_0 = 63$ deg on 2026-07 (Jupiter L5 and Neptune L4)

We define additional field centers at ecliptic longitudes $\beta = \beta_0 - 3.5$ deg and $\beta = \beta_0 + 3.5$ deg, where we assume each field center of LSST is shifted by 3.5 deg with respect to its neighbor. At each ecliptic longitude, we would have field centers at ecliptic latitude $\lambda = -3.5, 0.0, +3.5$ deg.

2.2 Observing Plan, Cadence, Filters, and Expected Depth

Our observing plan calls for 9 fields to be visited 8 times in a particular sequence: A, A + 2–3 days, B, B + 2–3 days, C, C + 2–3 days, D, D + 2–3 days. The conditions on these dates are that: A occur 1.5 months before opposition; B coincide as nearly as possible with a Jupiter and Neptune Trojan population conjunction and opposition; C occur 1.5 months after opposition; D coincide with the opposition of these fields 1 year after B. The ultimate reference point for this sequence will be B, which determines β_0 for our overall sequence, as well as the year in which this sequence begins.

On a given visit, all data should be taken back-to-back in the r -band filter. A total of 336 observations will allow detection of objects at $r = 27.0$ at 7 sigma, according to the LSST ETC¹. The *total* time requested for this plan is 9 fields, visited 8 times, each one with a sequence of 336 observations. This is a total of 24192 observations, which will be spread out over approximately 1 year. For comparison, we assume a nominal number of successful LSST visits per year of 268500². Looked at over a single year our request amounts to 9% of all successful observing time (even though our sequence takes slightly longer than a year, meaning the true fraction of observations is slightly lower).

2.3 Motivation for Proposed Fields

In terms of ecliptic latitude, the largest number of detections will take place for fields located near the ecliptic since the dominant populations (TNOs and MBCs) all have very peaked ecliptic latitude distributions. However, the Inner Oort Cloud bodies are expected to have significantly inclined populations when compared to the TNOs, which means that fields at high inclination are still useful for these populations. For the TNOs, we assume roughly a factor 3 drop in expected population at ecliptic latitudes of 3.5 degrees (Elliot et al., 2005). The main belt asteroids and thus the MBCs are a somewhat less inclined population, so we have assumed a factor 5 drop at 3.5 degrees ecliptic latitude. The inclination distribution of the Inner Oort cloud objects is unknown, but is likely to be considerably more inclined than the TNOs. Thus for these bodies, we have assumed a factor 2 drop in objects at 3.5 degrees ecliptic latitude. Sample populations are summarized in Table 1 based on the above observing scenario.

We include for comparison a reference survey with limiting magnitude of $r = 26.0$, which would only consume 16% the observing time as the proposal here. The fainter $r = 27.0$ survey finds approximately twice as many objects as the reference $r = 26.0$ survey, however these are expected to be the faintest, smallest and most distant bodies, and thus a target population uniquely available to LSST through deep drilling sequences.

2.3.1 Other Deep Drilling Cadences

We also outline considerations for DD fields that have been optimized for other LSST science. Since these are likely to be fixed for the duration of at least one season, we request they span a range

¹<http://dls.physics.ucdavis.edu:8080/etc4.3work/servlets/LsstEtc.html>

²http://opsimcvs.tuc.noao.edu/sample_survey.html

Table 1: Expected Deep Drilling Detections

Limiting Magnitude	Area [sq deg]	Main Belt Comets	Trans-Neptunians	Neptune Trojans	Inner Oort Cloud
26.0	86.4	150	1,060	6	9
27.0	86.4	280	2,200	16	20

This table includes estimates for LSST-detected Solar System populations, assuming the optimized deep drilling scenario described in the text. For reference, numbers for a shallower $r = 26.0$ limiting magnitude survey are given, along with numbers for the proposed survey depth of $r = 27.0$.

of ecliptic latitudes to probe the orbits of Inner Oort Cloud bodies, which are likely to be highly inclined. In addition, DD observing patterns lasting more than 2 years are not likely to be useful for Solar System science, as the orbits of most TNOs (aside from those entering/leaving the field of view during observations) will be sufficiently constrained with 2 years of data. The rapid motions of the more inner Solar System bodies means they will not spend significant amounts of time in a single field.

For the distant populations in particular, sequences of DD observations might plausibly be co-added using SAS over multiple nights. For instance, the difference in the parallactic motion over a week between a body at 975 AU (24.7 arcsec per week) and one at 1000 AU (24.1 arcsec per week) is about 0.6 arcsec at opposition, the typical seeing at the LSST site. Thus a week-to-week combination of observations is trivial to implement by placing a strict heliocentric distance limit on the orbits being surveyed. Even the motion over one month should be fairly trivial to survey as this would only correspond to a ~ 2.5 arcsec positional difference for objects at 975 AU compared to 1000 AU. As the only uncertainty is orbital motion, which is only of order a few arcsec as well, we believe SAS in static DD fields is a computationally tractable problem for a shell of bodies at ~ 1000 AU.

2.4 Observation-Time Cost

As outlined above, we are requesting 24192 observations over the timespan of approximately 1 year. This equates to approximately 9% of all observations taken by LSST in a year. This time request may be decreased by removing the fields at $\lambda = \pm 3.5$ deg.

3 Other Required or Relevant Observations

3.1 Other Required Observations

None

3.2 Other Relevant Observations

None

4 Specific Needs for LSST and for Deep Drilling

4.1 Need for LSST

It is very unlikely that a Solar System survey over several tens of square degrees, and down to $r = 27$, will be completed by the time LSST is on the sky. Even more so, it is unlikely that such

a survey will search for objects at such a wide range of distances (MBA to Inner Oort Cloud) as proposed here, and even more improbably that such a survey would have enough data to obtain well-measured orbits for the discovered objects. The size distribution for nearby objects, and the size distribution plus orbital distribution for distant objects, detectable using the combination of LSST’s deep drilling cadence plus shift-and-stack, will be entirely novel.

4.2 Need for Deep Drilling

A deep drilling cadence is required to achieve the extra depth required to image the smallest and most distant Solar System bodies. Our proposed visit profile – taking a series of continuous observations – is preferred for the SAS method as the computational complexity grows with the time separation of the images to be stacked as ΔT^3 . This makes having intra-night gaps in the data unfavorable.

5 Feasibility

5.1 General Feasibility

Shift-and-stack is a proven method to detect faint objects below the detection limit in a single image. The least computationally intensive means to implement SAS is to run a detection filter at the appropriate rates, as opposed to actually shifting and stacking the pixels (Fuentes et al., 2010). However, the number of shifts that must be probed scales as ΔT^3 , where ΔT is the time span of the data sequence (Bernstein et al., 2004). Therefore we limit the amount of data that will be used in SAS to a single nights deep drilling sequence, except for the most distant (~ 1000 AU) orbits which may be probed with adjacent night SAS. This constraint should be revisited in ~ 10 years when computational resources may have evolved sufficiently to enable multi-night SAS.

5.2 Bright Objects and Extinction

We prefer to avoid the Galactic plane for all DD sequences, to avoid the additional confusion and background noise provided by the Galactic disk and bulge populations. The confusion limit may be mitigated by using SAS on difference image, but the overall background noise levels will be elevated due to the background sources.

5.3 Unresolved Feasibility Issues

Shift-and-stack is not currently implemented in the LSST Data Management software stack. However, the “multi-fit” algorithm being developed for measurements of static objects in multiple epochs naturally provides a base infrastructure for this process. In particular, the marshaling of the pixels to attempt a given photometric measurement is non-trivial when tens of thousands of images are required. However, the multi-fit middleware is required to do exactly this, so we expect that this issue will be resolved by the time SAS is needed.

6 Other Issues

6.1 Relevance to LSST Commissioning

We strongly support the completion of one deep drilling sequence in the commissioning or first year of the survey. This will allow for tests of any systematics in the data at levels below what is available in single-epoch exposures, as well as provide an exemplary set of data to generate enthusiasm in the astronomical community for the upcoming decade of LSST observations.

6.2 Other Relevant Information

None

References

- Barbieri, C., Marchi, S., Migliorini, A., Magrin, S., Skvarč, J., Marzari, F., Scholl, H., & Albrecht, R. 2005, *Planetary and Space Science*, 53, 643
- Bernstein, G. M., Trilling, D. E., Allen, R. L., Brown, M. E., Holman, M., & Malhotra, R. 2004, *AJ*, 128, 1364
- Bottke, W. F., Morbidelli, A., Jedicke, R., Petit, J.-M., Levison, H. F., Michel, P., & Metcalfe, T. S. 2002, *Icarus*, 156, 399
- Brasser, R., Duncan, M. J., & Levison, H. F. 2006, *Icarus*, 184, 59
- Brown, M. E., Trujillo, C., & Rabinowitz, D. 2004, *ApJ*, 617, 645
- Dvorak, R., Bazzó, Á., & Zhou, L. 2010, *Celestial Mechanics and Dynamical Astronomy*, 107, 51
- Elliot, J. L., Kern, S. D., Clancy, K. B., Gulbis, A. A. S., Millis, R. L., Buie, M. W., Wasserman, L. H., Chiang, E. I., Jordan, A. B., Trilling, D. E., & Meech, K. J. 2005, *AJ*, 129, 1117
- Fraser, W. C., Brown, M. E., & Schwamb, M. E. 2010, *Icarus*, 210, 944
- Fuentes, C. I., Holman, M. J., Trilling, D. E., & Protopapas, P. 2010, *ApJ*, 722, 1290
- Gladman, B. & Chan, C. 2006, *ApJL*, 643, L135
- Gulbis, A. A. S., Elliot, J. L., Adams, E. R., Benecchi, S. D., Buie, M. W., Trilling, D. E., & Wasserman, L. H. 2010, *AJ*, 140, 350
- Hahn, J. M. & Malhotra, R. 2005, *AJ*, 130, 2392
- Harris, A. W. & Pravec, P. 2006, in *IAU Symposium*, Vol. 229, *Asteroids, Comets, Meteors*, ed. L. Daniela, M. Sylvio Ferraz, & F. J. Angel, 439–447
- Hsieh, H. H. 2007, PhD thesis, University of Hawai'i at Manoa
- Jedicke, R. & Metcalfe, T. S. 1998, *Icarus*, 131, 245
- Jewitt, D. 1996, *Earth Moon and Planets*, 72, 185
- Kaasalainen, M. & Torppa, J. 2001, *Icarus*, 153, 24
- Kaasalainen, M., Torppa, J., & Muinonen, K. 2001, *Icarus*, 153, 37
- Kaib, N. A. & Quinn, T. 2009, *Science*, 325, 1234
- Kenyon, S. J. & Bromley, B. C. 2004, *Nature*, 432, 598
- Kryszczyńska, A., La Spina, A., Paolicchi, P., Harris, A. W., Breiter, S., & Pravec, P. 2007, *Icarus*, 192, 223
- Levison, H. F., Duncan, M. J., Brasser, R., & Kaufmann, D. E. 2010, *Science*, 329, 187

- Lykawka, P. S., Horner, J., Jones, B. W., & Mukai, T. 2009, *MNRAS*, 398, 1715
- Mazzotta Epifani, E., Palumbo, P., Capria, M. T., Cremonese, G., Fulle, M., & Colangeli, L. 2008, *MNRAS*, 390, 265
- Morbidelli, A., Levison, H. F., Tsiganis, K., & Gomes, R. 2005, *Nature*, 435, 462
- Noll, K. S., Grundy, W. M., Stephens, D. C., Levison, H. F., & Kern, S. D. 2008, *Icarus*, 194, 758
- O'Brien, D. P. & Greenberg, R. 2005, *Icarus*, 178, 179
- Oort, J. H. 1950, *BAIN*, 11, 91
- Parker, A., Ivezić, Ž., Jurić, M., Lupton, R., Sekora, M. D., & Kowalski, A. 2008, *Icarus*, 198, 138
- Parker, A. H. & Kavelaars, J. J. 2010, *ApJL*, 722, L204
- Peale, S. J. 1993, *Icarus*, 106, 308
- Schwamb, M. E., Brown, M. E., Rabinowitz, D. L., & Ragozzine, D. 2010, *ApJ*, 720, 1691
- Sheppard, S. S. & Trujillo, C. A. 2006, *Science*, 313, 511
- . 2010, *ApJL*, 723, L233
- Snodgrass, C., Lowry, S. C., & Fitzsimmons, A. 2008, *MNRAS*, 385, 737
- Szabó, G. M., Kiss, L. L., & Sárneczky, K. 2008, *ApJL*, 677, L121
- Trujillo, C. A. & Brown, M. E. 2003, *Earth Moon and Planets*, 92, 99
- Tsiganis, K., Gomes, R., Morbidelli, A., & Levison, H. F. 2005, *Nature*, 435, 459